2018 International Conference on Indoor Positioning and Indoor Navigation (IPIN), 24-27 September 2018, Nantes, France

Super-Resolution in RSS-based Direction-of-Arrival Estimation

Thorsten Nowak, Markus Hartmann, Jörn Thielecke
Institute of Information Technology
Department Electrical, Electronic and Communication Engineering
Friedrich-Alexander University Erlangen-Nürnberg
Email: thorsten.nowak@fau.de

Niels Hadaschik, Christopher Mutschler
Machine Learning and Information Fusion Group
Locating and Communication Systems Department
Fraunhofer Institute for Integrated Circuits IIS, Nuremberg
Email: niels.hadaschik@iis.fhg.de

***Abstract*—For the evolving Internet-of-Things ubiquitous positioning is a core feature. Hence, energy- and location-awareness are essential properties of wireless sensor networks (WSNs). In terms low power consumption received signal strength (RSS)-based localization techniques outperform timing-based localization approaches. Therefore, RSS-based direction finding is prospective approach to location-aware, low-power sensor nodes. However, RSS-based direction-of-arrival (DOA) estimation is prone to multipath propagation. In this paper, a subspace-based approach to frequency-domain multipath resolution is presented. Resolution of multipath components allows for a RSS-based DOA estimation considering the power of the line of sight (LOS) component only. The impact of the multipath channel is considerably reduced with our approach. In contrast to common broadband DOA estimation techniques, the presented approach does not need phase-coherent receive channels or a synchronized sensor network. Hence, the proposed super-resolution technique is applicable to low-power sensor networks and brings accurate positioning to small-sized and energy-efficient sensor nodes.**

I. Introduction

In recent years there has been significant progress in locating wireless sensor networks (WSNs). Lately, WSNs have become popular in many applications and localization has become a core feature of modern WSNs [1], [2]. WSNs successfully address applications such as animal tracking [3], [4], smart metering [5], and collision avoidance [6]. What they all have in common is that the sensor information is meaningless without any location information. Hence, positioning capability is the most important feature of today's sensor networks.

Phased arrays are the most common approach to radio-based direction-of-arrival (DOA) estimation [7]. However, utilizing phased arrays for DOA estimation demands for coherent and calibrated receive channels. Time-of-flight–based systems, like the Global Navigation Satellite System (GNSS), require precisely synchronized nodes and power-intensive signal processing. This prevents their application to low-cost applications and low-power systems. An approach to circumvent the need of coherent receive channels and network synchronization is to use power measurements. In this paper we focus on received signal strength (RSS)-based direction finding. There are numerous approaches to RSS-based DOA in literature. They use multiple directional antennas [8], [9], a single rotating antenna [10], [11] or active reflectors [12]. Instead of mechanically moving the antenna, there are approaches that use switched beam antennas as presented in [13]. Another approach is applying electronically steerable parasitic array radiator antennas [14]. Recently, multi-mode antennas have been investigated for power-based DOA estimation [15]. Also a variant of the MUltiple SIgnal Classification (MUSIC) algorithm for power measurements has been proposed in [16]. Theoretical limits in RSS-based direction finding have been discussed in [9].

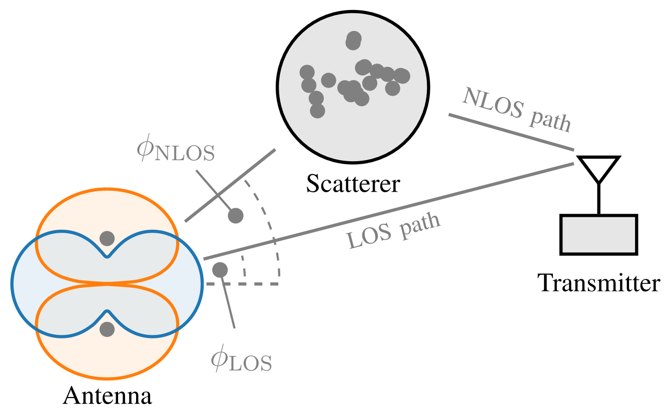

Fig. 1. Radio propagation channel with single scatterer cluster. Radio signals are scattered by objects, e.g., trees. Scattering spreads power in the angular domain inherently degrading DOA estimates. The above radio propagation scenarios features two resolvable propagation paths: the LOS component and a NLOS component. In general, the NLOS component significantly affects RSS measurements. Hence, RSS-based DOA estimation is impaired in multipath scenarios.

However, multipath propagation is still one of major issues in radio-based localization. Also RSS-based DOA suffers severely from multipath propagation caused by scattering. Figure 1 exemplary depicts a two-path propagation channel. When directed antennas are considered in presence of multipath propagation RSS measurements are impaired. Probabilistic approaches to multipath mitigation in power-based direction finding such as [17] are limited as they require prior knowledge of statistical channel parameters. Furthermore, such multipath mitigation techniques significantly increase the variance of DOA estimates as a cost of unbiasedness. In this paper, we present a super-resolution multipath mitigation technique to

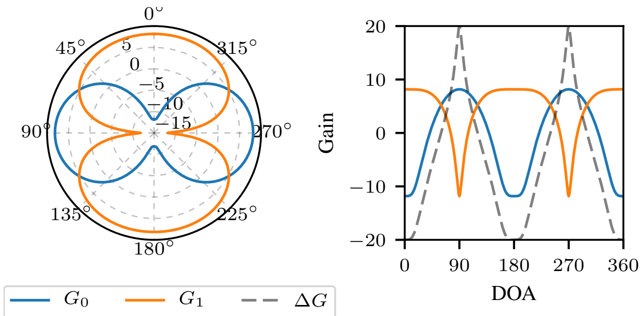

Fig. 2. Radiation power patterns for perfect dipole antennas in horizontal plane for in phase and out of phase coupling. To meet realistic scenarios the antenna elements exhibit mutual cross coupling at a level of -20 dB.

RSS-based DOA.

The paper is organized as follows. A review of RSS-based DOA is given in Section II. In Section III the impact of the wireless propagation channel is described. We introduce Delay estimation applying the MUSIC algorithm on channel transfer functions (CTFs) in Section IV. The method of multipath component (MPC) power estimation utilizing time-shifted signal replicas is presented in Section V. In Section VI the approach to probabilistic multipath mitigation presented in [17] is recapitulated. Exhaustive Monte Carlo simulations show the potential of the proposed super-resolution approach to RSS-based DOA estimation in Section VII. Section VIII concludes the paper.

II. Review of RSS-based DOA

For this paper we consider RSS-based DOA estimation applying coupled dipole antennas [9]. Furthermore, it is assumed that localization takes place in the horizontal plane orthogonal to the two dipoles. Presuming a perfect linear dipole array, the radiation of the dipoles in the horizontal plane (i.e., $\theta = 90°$) is constant over all impinging signal angles in azimuth $\phi \in [0, 2\pi]$. Hence, the radiation pattern for N dipoles is given by the array factor [18]

$$AF = \sum_{i=0}^{N-1} c_i \cdot \exp(-j \cdot 2\pi \sin(\theta) \cdot d_i \cos(\phi)), \tag{1}$$

where d_i are the corresponding distances of the dipole elements, λ is the wavelength, and c_i is the coupling factor. Considering only two dipoles at distances $d_0 = 0$ and $d_1 = d$ and $\theta = 90°$ the array factor reduces to

$$AF = c_0 + c_1 \cdot \exp(-j \cdot 2\pi \cdot d \cos(\phi)). \tag{2}$$

For the considered antenna array the dipoles are coupled in phase and out of phase, respectively. Hence, the radiation patterns are given by

$$g_0(\phi) = 1 + \exp(-j2\pi d \cdot \cos(\phi)), \text{ and} \tag{3}$$
$$g_1(\phi) = 1 - \exp(-j2\pi d \cdot \cos(\phi)). \tag{4}$$

We define the radiation power patterns $G_a(\phi)$ (in dB) by

$$G_a(\phi) = 10 \lg |g_a(\phi)|^2 . \tag{5}$$

The gain difference function of the described antenna array is expressed by

$$\Delta G(\phi) = G_1(\phi) - G_0(\phi). \tag{6}$$

The radiation power patterns for the antenna array at hand and the gain difference function are depicted in Figure 2.

The RSS at a receiver a for a transmitted signal with power P_{TX} can be computed as follows

$$P_{\mathrm{RX},a} = P_{\mathrm{TX}} - L + G_{\mathrm{TX}} + G_a(\phi) + w_a, \tag{7}$$

with L denoting the bulk path loss. G_{TX} and $G_a(\phi)$ are transmit and receive antenna gain, respectively. When considering a single signal source, i.e., no multipath propagation, the received signal strength difference is given by

$$\Delta P_{\mathrm{RX}} = \Delta G(\phi) + w, \tag{8}$$

due to the fact that both channels are stimulated by the same transmit power and exhibit equal path loss. Thus, the gain difference function does not depend on transmit power and path loss. Hence, it may be estimated without prior knowledge of the the path loss exponent and the power emitted by the transmitter. This fact is, in contrast to range-based localization based on RSS, a major benefit of RSS-based DOA estimation.

The above consideration hold for the absence of multipath propagation. In case of multiple MPCs the observed difference in signal strength is not linked to the DOA of the line of sight (LOS) component. Hence, in general the direction of the LOS signal may not be inferred from RSS difference without further effort. In [17] an approach to probabilistic multipath mitigation has been presented. However, this mitigation technique is only applicable if prior knowledge of stochastic channel parameters, e.g., the angular spread (AS), is available. Furthermore, this approach allows only for mean-free DOA estimates on a statistical average. Besides that, the variance of the DOA estimates significantly increases if this technique is applied in presence of severe multipath propagation. Thus, probabilistic multipath mitigation is only feasible in moderate multipath scenarios.

III. Wireless Channel Model

Any radio-based localization system is affected by impairments of the wireless radio propagation channel. However, in real-world use cases there is a severe impact of the radio channel as objects, e.g., in industrial environments, cause reflections, refraction, diffraction and blockages. Hence, in practice we must consider a multipath channel. We introduce the channel model as follows.

In general, the impulse response h of a wireless channel can be described by a tapped delay line [19]

$$h = \sum_{l=1}^{L} a_l \cdot \delta(t - \tau_l), \tag{9}$$

with a_l being the complex coefficient of the l-th MPC and τ_l its respective delay for a channel with L propagation paths. For channel simulation and verification of the proposed

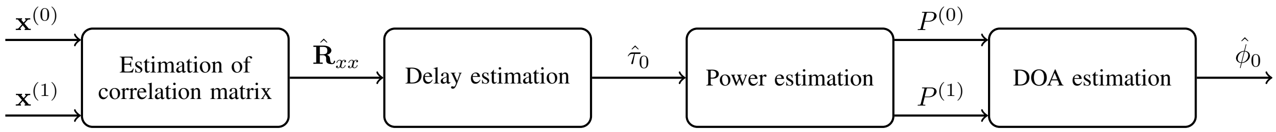

Fig. 3. Signal processing blocks: The correlation matrix $\widehat{\mathbf{R}}_x x$ is estimated from data, i.e., measured CTFs for two receive paths. Afterwards, delays τ_l and respective powers P_l are estimated. Finally, the arrival angle $\widehat{\phi}_0$ is estimated from the powers of the LOS component.

algorithms QuaDRiGa [20] is used to model the wireless propagation channel. We briefly outline the procedure of channel simulation here. From large-scale parameters (LSPs), i.e., amongst others number of dominant paths L, delay spread and angular spread, a channel impulse response of a specific channel realization is computed. This comprises the following steps:

1) Draw delays τ_l
2) Compute powers P_l
3) Draw arrival angles ϕ_l
4) Combine above to channel coefficients a_l

Given the complex channel coefficients and the corresponding delays and signal directions the received power incorporating the antenna gain can be computed as follows [17]

$$P_a = 10 \lg \left| \sum_{l=1}^{L} g_a(\phi_l) \cdot a_l \right|^2 , \qquad (10)$$

where $g_a(\phi_l)$ is the amplitude gain of the considered antenna for an arrival angle ϕ_l. Recalling the RSS-based DOA estimation presented in the previous and (6), the RSS difference for the multipath channel at hand is defined by

$$\Delta P_a = 10 \lg \left| \sum_{l=1}^{L} g_1(\phi_l) \cdot a_l \right|^2 - 10 \lg \left| \sum_{l=1}^{L} g_0(\phi_l) \cdot a_l \right|^2 . \qquad (11)$$

The impact of multipath propagation on the RSS difference and thus the DOA estimates has been extensively discussed in [17]. Multipath propagation leads to a large bias in DOA estimates.

IV. Super-Resolution in RSS-based DOA

In this paper, we present a super-resolution approach to power-based DOA estimation in multipath environments. As the antenna array considered in this work only features two receive ports, there is no probability to cancel multipath effects in the spatial domain. Hence, we propose a method to separate the individual MPCs in the frequency domain. MPC delays are resolved by applying super-resolution techniques on measured CTFs [21]. The MPC power is estimated from the sample covariance matrix of the measured CTFs. Subsequently, the method of RSS-based DOA estimation described in Section II can be applied to the power of LOS component. Based on the LOS power estimate, impairments due to multipath propagation can be significantly reduced. An overview of the signal processing blocks is given in Figure 3. In the sequel of this section, spectral analysis in general is reviewed and adapted to CTF measurements. Furthermore, spatial smoothing and model-order selection are covered in this section.

A. Signal Model and Spectral Analysis

For the delay estimation spectral signals analysis is applied [21]. More specifically, the MUSIC algorithm [22] is used to estimate the delays of the dominant MPCs. We are considering noisy time signals $x(t)$ that are modeled as a superposition of complex sinusoids. The sum of complex sinusoids is given by

$$x(t) = a(t) + w(t) = \sum_{k=1}^{K} \alpha_k e^{j(\omega_k t + \varphi_k)} + w(t), \qquad (12)$$

where $w(t)$ is a additive white Gaussian noise (AWGN) process with variance σ_w^2. The complex sinusoids are characterized their angular frequency ω_k, amplitude α_k and phase φ_k. Introducing the following very common notation [21]

$$\begin{aligned} \mathbf{v}(\omega) &= \begin{bmatrix} 1 & e^{-j\omega} & \dots & e^{-j(M-1)\omega} \end{bmatrix}^T \\ \mathbf{V} &= \begin{bmatrix} \mathbf{V}(\omega_1) & \dots & \mathbf{V}(\omega_m) \end{bmatrix}, \end{aligned} \qquad (13)$$

with (13) the sample vector $\mathbf{x}(t)$ may be written as

$$\begin{aligned} \mathbf{x}(t) &= \begin{bmatrix} x(t) & x(t-1) & \dots x(t-M+1) \end{bmatrix}^T \\ &= \mathbf{V}\mathbf{a}(t) + \mathbf{w}(t). \end{aligned} \qquad (14)$$

$\mathbf{w}(t)$ composes the noise contribution and $\mathbf{a}(t)$ complex sinusoids satisfying $a_k(t) = \alpha_k e^{j(\omega_k t + \varphi_k)}$. Signal vector and noise vector are given by

$$\begin{aligned} \mathbf{a}(t) &= \begin{bmatrix} a_1(t) & \dots & a_m(t) \end{bmatrix}^T \\ \mathbf{w}(t) &= \begin{bmatrix} w(t) & \dots & w(t-M+1) \end{bmatrix}^T . \end{aligned} \qquad (15)$$

The sample covariance matrix $\mathbf{R}_{xx}$ for $\mathbf{x}(t)$ is defined by

$$\mathbf{R}_{xx} = \mathcal{E}\left\{\mathbf{x}(t)\mathbf{x}^H(t)\right\} = \mathbf{V}\mathbf{A}\mathbf{V}^H + \sigma_w^2 \mathbf{I} \qquad (16)$$

$$\text{with } \mathbf{A} = \operatorname{diag}\left(\alpha_1^2, \dots, \alpha_m^2\right), \qquad (17)$$

where $\mathbf{I}$ is the identity matrix and σ_w^2 the noise variance of $w(t)$. Eigenvalue decomposition of $\mathbf{R}$ results in real-valued Eigenvalues $\lambda_1 \geq \lambda_2 \geq \dots \geq \lambda_M$. The corresponding Eigenvectors are separated into two groups. Eigenvectors $\{\lambda_1, \dots, \lambda_n\}$ and $\{\lambda_{n+1}, \dots, \lambda_M\}$ are denoted by $\{\mathbf{s}_1, \dots, \mathbf{s}_n\}$ and $\{\mathbf{g}_1, \dots, \mathbf{g}_{M-n}\}$, respectively. The Eigenvectors are composed to the matrices

$$\mathbf{S} = [\mathbf{s}_1, \dots, \mathbf{s}_n] \qquad \mathbf{G} = [\mathbf{g}_1, \dots, \mathbf{g}_{M-n}] . \qquad (18)$$

It can be shown that

$$\operatorname{rank}(\mathbf{V}\mathbf{A}\mathbf{V}^H) = n. \qquad (19)$$

Thus, $\mathbf{VAV}^H$ has exactly n positive Eigenvalues and $(M-n)$ Eigenvalues equal to zero. For $\left\{\tilde{\lambda}_1,\ldots,\tilde{\lambda}_M\right\}$ being the Eigenvalues of $\mathbf{VAV}^H$, the Eigenvalues of $\mathbf{R}$ become

$$\lambda_k = \tilde{\lambda}_k + \sigma_w^2 \qquad (k=1,\ldots,m). \tag{20}$$

Considering noisy samples, we can state

$$\begin{cases}\lambda_k > \sigma_w^2 & \text{for } k=1,\ldots,n\\ \lambda_k = \sigma_w^2 & \text{for } k=n+1,\ldots,M\end{cases}. \tag{21}$$

Considering (16) and (21), we can reformulate

$$\mathbf{RG} = \mathbf{G}\cdot\operatorname{diag}\left(\lambda_{n+1}\ldots,\lambda_M\right) = \mathbf{VAV}^H\mathbf{G} + \sigma_w^2\mathbf{G}, \tag{22}$$

which finally leads to the orthogonality condition

$$\mathbf{V}^H\mathbf{G} = 0. \tag{23}$$

Thus, columns of $\mathbf{G}$, i.e., the Eigenvectors $\mathbf{g}_k$, belong to the kernel of $\mathbf{V}^H$. Since $\operatorname{rank}(\mathbf{A}) = n$, the dimension of $\mathcal{N}(\mathbf{V}^H)$ is $m-n$ which equals the dimension of the column space of $\mathbf{G}$.

$$\mathcal{R}(\mathbf{G}) = \mathcal{N}(\mathbf{V}^H) \tag{24}$$

Hence, the subspace $\mathcal{R}(\mathbf{G})$ is called noise subspace. Deducing from (23), the true frequencies $\{w_k\}_{k=1}^n$ are the only solutions to

$$\mathbf{v}^H(\omega)\mathbf{GG}^H\mathbf{v}(\omega) = 0 \quad \text{for any } m>n. \tag{25}$$

B. MUSIC Algorithm

In real-world estimation problems the covariance matrix $\mathbf{R}_{xx}$ is not known. Therefore, it has to be estimated from the signal samples

$$\hat{\mathbf{R}}_{xx} = \frac{1}{N}\sum_{i=1}^{N}\mathbf{x}_i(t)\mathbf{x}_i^H(t). \tag{26}$$

Subsequently, the Eigenvalues and Eigenvectors of $\hat{\mathbf{R}}$ are computed composing the matrices $\hat{\mathbf{S}}$ and $\hat{\mathbf{G}}$. Briefly, two MUSIC variants are described below:

Spectral MUSIC Yields good visual interpretation as a *pseudospectrum* and is computed by maximizing

$$\frac{1}{\mathbf{v}^H(\omega)\hat{\mathbf{G}}\hat{\mathbf{G}}^H\mathbf{v}(\omega)} \qquad \omega\in[-\pi,\pi] \tag{27}$$

for all ω_k. Spectral peaks correspond to the frequencies ω of the sinusoidal components.

Root MUSIC In this case, the solution to (25) is computed analytically substituting $e^{j\omega}$ by z, the problem at hand is expressed by

$$\mathbf{v}^H(z^{-1})\hat{\mathbf{G}}\hat{\mathbf{G}}^H\mathbf{v}(z) = 0, \tag{28}$$

where $\mathbf{V} = [\mathbf{v}(\omega_1),\ldots,\mathbf{v}(\omega_m)]$. In this computationally very efficient approach the roots of the polynomial on the left hand side of (28) closest to the unit circle are chosen.

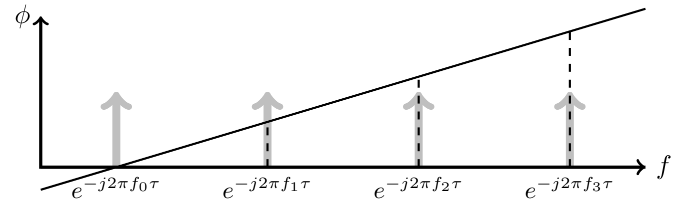

Fig. 4. Delay estimation with discrete CTFs. In this figure a single path with delay τ is considered. The delay results in phase ramp $\phi = \arg(H(f)) \propto f$. The CTF is sampled at discrete frequencies indicated by the diracs.

C. Delay Estimation Utilizing CTFs

Analogously to DOA estimation applying uniform linear arrays (ULAs), cf. Figure 4, we consider delay estimation applying multitone signals. Multitone signals may be easily realized by orthogonal frequency-division multiplexing (OFDM) or repeated m-Sequences. Regardless of the specific realization of the multitone signal, the essential property is its capability of uniform sampling of the frequency space. Hence, applying multitone signals allows for determination of a discrete CTF.

The delays of the MPCs can be recovered from discrete CTFs, cf. [23]. The measurement data is obtained by sampling the CTF at M equally spaced frequencies. We are considering a single sample $x(m)$ of a CTF $H(f)$ at a distinct frequency f_m. All signal impairments are summarized in a single AWGN process $w(l) \sim N(0,\sigma_w^2)$. A single sample is computed by superposition of the CTFs of the MPC

$$x(m) = H(f_m) + w(m) = \sum_{l=1}^{L}\alpha_k e^{-j2\pi f_m\tau_l} + w(m). \tag{29}$$

Defining the sampled discrete frequencies by $f_m = f_0 + m\Delta f$, where f_0 is the lowest subcarrier frequency. The samples of the M subcarriers may be stacked to data vector $\mathbf{x}$ expressed by

$$\mathbf{x} = \mathbf{H} + \mathbf{w}, \tag{30}$$

where

$$\mathbf{x} = \begin{bmatrix}x(0) & x(1) & \ldots & x(M-1)\end{bmatrix}^T \tag{31}$$

$$\mathbf{H} = \begin{bmatrix}H(f_0) & H(f_1) & \ldots & H(f_{(M-1)})\end{bmatrix}^T \tag{32}$$

$$\mathbf{w} = \begin{bmatrix}w(0) & w(1) & \ldots & w(M-1)\end{bmatrix}^T \tag{33}$$

Decomposing $\mathbf{H}$ in vector form, we can write

$$\mathbf{x} = \mathbf{Va} + \mathbf{w} \tag{34}$$

where

$$\mathbf{V} = \begin{bmatrix}\mathbf{v}(\tau_0) & \mathbf{v}(\tau_1) & \ldots & \mathbf{v}(\tau_{(L-1)})\end{bmatrix}^T \tag{35}$$

$$\mathbf{v}(\tau_k) = \begin{bmatrix}1 & e^{-j2\pi\Delta f\tau_k} & \ldots & e^{-j2\pi(M-1)\Delta f\tau_k}\end{bmatrix}^T \tag{36}$$

$$\mathbf{a} = \begin{bmatrix}\alpha_0 e^{-j2\pi f_0\tau_0} & \alpha_1 e^{-j2\pi f_0\tau_1} & \ldots & \alpha_{L-1}e^{-j2\pi f_0\tau_{(L-1)}}\end{bmatrix}^T \tag{37}$$

Delays are estimated applying the MUSIC super-resolution technique based on the Eigenvalue decomposition of the autocorrelation matrix

$$\mathbf{R}_{xx} = \mathcal{E}\left\{\mathbf{x}\mathbf{x}^H\right\} = \mathbf{V}\mathbf{A}\mathbf{V} + \sigma_w \mathbf{I} \tag{38}$$

as described in Section IV-A. We assume that magnitude of α_k is constant and the phase is uniformly distributed. Thus, matrix $\mathbf{A}$ is nonsingular. Comparing the signal models described in the MUSIC section, delays are retrieved from estimated frequencies by

$$\tau_l = \frac{\omega_l}{2\pi\Delta f}. \tag{39}$$

In order to avoid spatial aliasing the maximum delay is limited by $2\tau_{\max} \leq 1/\Delta f$.

D. Spatial Smoothing

When considering multipath scenarios signals are not uncorrelated as MPCs are just scaled, phase shifted and delayed replicas of the transmitted signal. In consequence, the rank of the matrix $\mathbf{V}\mathbf{A}\mathbf{V}^H$ is reduced to one. This contradicts with requirement $\mathrm{rank}(\mathbf{V}\mathbf{A}\mathbf{V}^H) = L$. Hence, spectral estimates usually are strongly biased without further effort in presence of multipath propagation. To cope with coherent signals preprocessing schemes, e.g., Forward Backward Spatial Smoothing (FBSS), have been developed that allow for decorrelation of the estimated correlation matrix. Applying FBSS guarantees that $\widehat{\mathbf{A}}$ is full-rank [24]. Another advantage of this procedure is that a single CTF sample is sufficient. This is not obvious as for a single sample the assumption of α_k having uniform distribution does not hold true [23].

Spatial smoothing has been described in-depth in [24]. The data vector of length M is divided in $M-N+1$ overlapping vectors of size N

$$\mathbf{x}_n = \begin{bmatrix} x(n) & x(n+1) & \dots & x(n+M-1) \end{bmatrix} \tag{40}$$
$$\text{with } n = 1, 2, \dots, M-N+1.$$

For the corresponding covariance matrices $\mathbf{R}_n$ the forward correlation matrix $\mathbf{R}^f$ is computed by

$$\mathbf{R}^f = \frac{1}{M-N+1} \sum_{l=1}^{M-N+1} \mathbf{R}_n^f \tag{41}$$

The estimate of the correlation matrix can be improved applying forward-backward averaging

$$\widehat{\mathbf{R}}^{fb} = \frac{1}{2}(\mathbf{R}^f + \mathbf{J}\left[\mathbf{R}^f\right]^* \mathbf{J}), \tag{42}$$

where

$$\mathbf{J} = \begin{bmatrix} 0 & & 1 \\ & \iddots & \\ 1 & & 0 \end{bmatrix}. \tag{43}$$

It can be shown that $\widehat{\mathbf{R}}^{fb}$ has full-rank and, thus, allows to apply spectral estimation. However, the dimension of the covariance matrix is reduced from $M \times M$ to $N \times N$. Hence, the number of MPCs must fulfill $L < N-1$ in order separate the components. Practical implementations [23] consider values from $M/3$ to $3M/4$ for N.

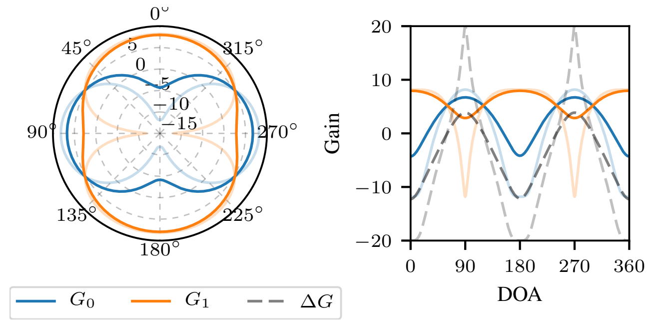

Fig. 5. Channel-adaptive radiation power patterns and effective gain difference function. The light lines denote the orignal radiation power patterns without any multipath compensation. Obviously, the gain difference function is flattenen by spreading the energy of the impinging signals in the spatial domain.

E. Model-Order Selection

In the previous sections we assumed the number of MPCs to be known. However, in real-world radio propagation channels this is not the case. Nevertheless, knowledge of the model order, i.e., number MPCs, is essential for the use of super-resolution techniques. Prior to delay estimation the number of signal components has to be estimated from the Eigenvalue decomposition of the sample correlation matrix. In theory all noise Eigenvalues are equal to the noise variance. Since the correlation matrix is an estimated one this assumption does not hold true. Commonly, information theoretic criteria are used for the estimation of the model order. In [25], information theoretic criteria are introduced for model order selection. In this paper, the minimum description length (MDL) criterion [26] is utilized, which is defined by

$$\mathrm{MDL}(\tilde{L}) = -\ln\left(\frac{\prod\limits_{k=\tilde{L}_p+1}^{M} \hat{\lambda}_k^{1/M-\tilde{L}}}{\frac{1}{M-\tilde{L}}\sum\limits_{k=\tilde{L}_p+1}^{M} \hat{\lambda}_k}\right)^{N(M-\tilde{L})} \tag{44}$$

$$+ \frac{\tilde{L}}{4} \cdot (2M - \tilde{L} + 1) \cdot \ln N \tag{45}$$

The second term is modified from the standard MDL criterion for the application of FBSS [27]. The estimated model order $\tilde{L}$ is found minizing

$$\hat{L}_P = \underset{\tilde{L}}{\mathrm{argmin}}\, \mathrm{MDL}(\tilde{L}), \tag{46}$$

where M denotes the number of Eigenvalues $\hat{\lambda}_k$ and N is the number of samples that have been used for the estimation of the correlation matrix.

V. MPC Power Estimation

In the section above, the procedure of delay estimation has been described applying super-resolution techniques. Each MPC is characterized by its delay τ_l and its complex amplitude

a_l. In [28] a time-domain approach to the estimation of delays and complex amplitudes is proposed. For the subspace-based approach presented here, since second order statistics comprise non phase information, only the absolute values of the amplitude can be recovered from the sample covariance matrix [29]. For a measured CTF $\widehat{\mathbf{H}}$ the delay estimates τ are found applying the MUSIC algorithm. For each delay τ_l a corresponding normalized CTF $\widehat{\mathbf{H}}_\mathbf{l}$ is computed by

$$H_l(f) = e^{-j2\pi f \tau_l}. \tag{47}$$

In absence of noise the CTF $\widehat{\mathbf{H}}$ is a linear combination of the individual CTFs of the delay multipaths given by

$$\widehat{\mathbf{H}} = \sum_{l=1}^{L} a_l \widehat{\mathbf{H}}_l \tag{48}$$

which can be written in matrix from

$$\widehat{\mathbf{H}} = \widehat{\mathbf{H}}_{\mathrm{MPC}} \mathbf{a}, \tag{49}$$

with $\widehat{\mathbf{H}}_{\mathrm{MPC}} = [\widehat{\mathbf{H}}_1, \ldots, \widehat{\mathbf{H}}_L]$. The solution to the problem stated in (49) can be found be the well-known linear least squares approach by minimizing the quadratic error for the respective channel estimates $\widehat{\mathbf{H}}$ and $\widehat{\mathbf{H}}_{\mathrm{MPC}}$

$$\widehat{\mathbf{a}} = \underset{\mathbf{a}}{\mathrm{argmin}} \left\| \widehat{\mathbf{H}} - \widehat{\mathbf{H}}_{\mathrm{MPC}} \mathbf{a} \right\|_2^2. \tag{50}$$

Finally, MPC powers are computed by

$$\widehat{\mathbf{P}} = \begin{bmatrix} |\widehat{\mathbf{a}}_1|^2 \\ \vdots \\ |\widehat{\mathbf{a}}_L|^2 \end{bmatrix}. \tag{51}$$

Decomposing the CTF into single MPCs the LOS path can be extracted. The power allocated to the path with the shortest delay, i.e., the LOS path, can be utilized for RSS-based direction finding technique described in Section II.

VI. Probabilistic Multipath Mitigation

The probabilistic multipath mitigation technique presented in [17] is briefly reviewed in this section. The effect of multipath propagation, more specifically the angular spread of the impinging signal, has been characterized by (10) in Section III. In fact, the AS results in compression of the gain functions of the directed antennas. Thus, its effect is most severe at the extrema of the gain difference function. This leads to a large bias in DOA estimates, especially at multiple of 90°. In order to compensate for the AS channel-effective gain patterns can be computed that consider the multipath channel on a statistical basic. In the spatial domain the multipath channel is characterized by its AS. With a-priori knowledge of the AS its impact may be mitigated on average by applying modified gain pattern. The effective gain patterns are computed by

$$|g_{\mathrm{MP}}(\phi)|^2 = |g(\phi)|^2 * p_{\mathrm{AS}}(\phi), \tag{52}$$

with $*$ denoting a circular convolution and the probability density function (PDF) of the angular spread given by

$$p_{\mathrm{AS}}(\phi) = \mathrm{N}(0, \sigma_{\mathrm{AS}}^2). \tag{53}$$

Note that the gain functions are non-logarithmic scale here. Exemplary the effective patterns are depicted for an AS of $\sigma_{\mathrm{AS}} = 25°$ in Figure 5. It can be easily seen that the dynamic range of the effective gain difference function is significantly reduced. However, the effective gain difference function resembles the average RSS measurements for the corresponding LOS arrival angles of the considered signal source in presence of multipath. Hence, utilizing the effective patterns allows for DOA estimates with significantly reduced bias. Nevertheless, a downside of this probabilistic approach is that the variance of the DOA estimates is increased. Although estimates are unbiased on average, a single realization of a multipath channel results in biased DOA estimates which inherently increases the variance of the DOA estimates. Furthermore, it has to be noted that the DOA estimator, as presented in [9] is biased in general.

VII. Results

For the verification of the presented approach exhaustive Monte Carlo simulations have been run utilizing the QuaDRiGa channel model [20]. The focus is on the impact of the LSP channel AS. As shown in [17] the impairments due to multipath propagation increase in RSS-based DOA for increasing angular spread. In the sequel, we consider four different algorithms for the estimation of the DOA of the impinging signal. These are

1) RSS-based DOA (DRSS) [9]
2) Probabilistic multipath mitigation for RSS-based DOA (PMM) [17]
3) Power-based DOA with super-resolution of LOS component (SR)
4) Power-based DOA with super-resolution of LOS component and spatial diversity (SRD).

The DRSS approach is classic RSS-based direction finding without any multipath mitigation at all. With the PMM method the multipath effects are to be canceled based on prior statistical channel information. Both super-resolution techniques (SR/SRD) consider multipath resolution in the frequency domain in order to extract the LOS component. For the SR method delays are computed for the two receive channels individually, whereas for the SRD method delays are estimated based on the CTFs captured by both receive channels. Hence, the SRD approach has a slight diversity gain compared to the SR method. However, the SRD method demands for time-synchronized receive channels. Algorithms are benchmarked by a set of Monte Carlo runs that simulate a large number of channel realizations for a multipath channel with an AS of $\sigma_{\mathrm{AS}} = 25°$. This procedure has been extensively discussed in [17] and has been reviewed in Section III and Section VI. The most essential channel parameters have been set to the following:

- Angular spread: $\sigma_{\mathrm{AS}} = 25°$

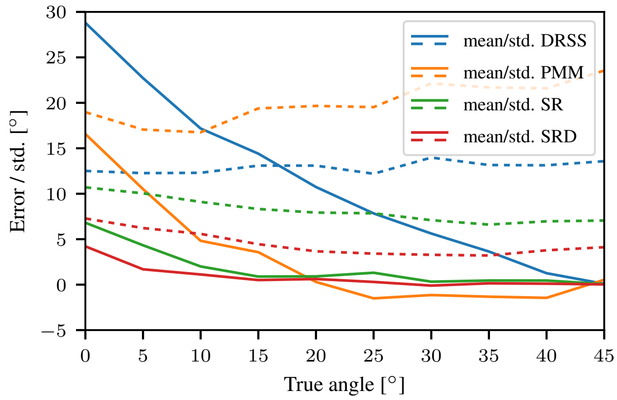

Fig. 6. Mean error and standard deviation for LOS angles $\phi_{\mathrm{LOS}} \in [0°, 45°]$. Obviously, the DRSS algorithm is severely biased. By incorporating prior channel knowledge, the PMM allows for a significant reduction of the bias at the cost of an increased variance. Applying super-resolution techniques (SR/SRD) drastically reduces bias and variance by resolving the individual propagation paths. SRD slightly improves the estimates compared to SR by exploitation of spatial diversity.

- Bandwidth: $B = 40\,\mathrm{MHz}$
- Number of carriers: 31
- SNR: $\mathrm{SNR} = 30$
- RMS delay spread: $\sigma_\tau = 50\,ns$
- Number of MPCs: $L = 6$
- K-factor: $K = 1$

In Figure 6 the estimation results for the four DOA estimators are shown. Mean errors are denoted by solid lines and the corresponding standard deviations by dashed lines. Apparently, the estimates for the DRSS method are biased. Due to the nature of the gain difference function this effect is worst at multiple of 90°. Hence, the bias increases significantly for LOS angles closer to 0°. Without any mitigation RSS-based DOA estimation (DRSS) is very erroneous in multipath environments. For the probabilistic multipath mitigation approach (PMM) proposed in [17] it can be seen that the bias drastically reduces. However, the PMM method is still biased. Nevertheless, it has to be noted that this bias does not inherently arise from the multipath channel, but is an artifact of the utilized estimator. The channel-adapted gain patterns utilized by the PMM method perfectly resemble the multipath channel on average. Though, the AS results in increased variance of the RSS difference measurements. This inherently leads to biased estimates when the Maximum Likelihood (ML) estimator is considered for RSS-based direction finding. Error bounds for the ML estimator have been discussed in detail in [9]. Another drawback of the probabilistic mitigation approach is the increased variance of the DOA estimates. Both super-resolution techniques (SR/SRD) show zero-mean DOA estimates and a considerable decrease in the variance of the DOA estimates. Due to spatial diversity the SRD method slightly outperforms the SR method. Especially for the nulls of the antenna pattern delay estimates are less robust due the large attenuation close to multiples of 90°. In these regions there is a substantial spatial diversity gain in the robustness of the delay estimates.

In Figure 7 and Figure 8 the distribution of DOA estimates is shown for a LOS angle of 30° and 45°, respectively. Once again, the DOA estimates for DRSS method are biased for a LOS angle of 30°, whereas the PMM approach allows for mean-free estimates. There is no bias for a LOS angle of 45° as the AS is not harmful in this region of the gain difference pattern. Hence, there is no performance gain when applying the PMM method. In fact, rather the opposite is true. Applying PMM slightly increases the variance of the estimated DOAs. The super-resolution techniques (SR/SRD) feature zero-mean angle estimates and a drastically reduced variance. Exploiting spatial diversity (SRD) results in more robust delay estimates. Thus, variance slightly decreases compared to the SR method.

VIII. Conclusion

In this paper, we proposed super-resolution methods for power-based direction finding. Spectral analysis has been reviewed and adopted to CTF measurements. The presented approach considers multipath resolution in the frequency domain and allows for isolation and identification of the LOS component of a multipath propagation channel. An approach to MPC power estimation has been presented utilizing the sample covariance matrix of CTF measurements.

Furthermore, spatial diversity has been exploited in order to enhance delay estimates. Robust delay estimates result in slightly more accurate DOA estimates. However, the diversity approach requires time-synchronized receive channels. Both super-resolution methods outperform probabilistic mitigation techniques. Moreover, the presented super-resolution approach does not depend on prior channel knowledge, which in this case would an estimate of the AS. Therefore, the presented frequency domain multipath resolution approach makes RSS-based DOA estimation applicable in multipath scenarios for small-size, low-power sensor networks.

Acknowledgment

This work is funded by the German Science Foundation DFG grant FOR 1508, Research Unit BATS.

References

[1] J. Hightower and G. Borriello, "Location systems for ubiquitous computing," *Computer*, vol. 34, pp. 57–66, Aug 2001.

[2] M. Vossiek, L. Wiebking, P. Gulden, J. Wieghardt, C. Hoffmann, and P. Heide, "Wireless local positioning," *IEEE Microwave Magazine*, vol. 4, pp. 77–86, Dec 2003.

[3] R. Kays, S. Tilak, M. Crofoot, T. Fountain, D. Obando, A. Ortega, F. Kuemmeth, J. Mandel, G. Swenson, T. Lambert, B. Hirsch, and M. Wikelski, "Tracking animal location and activity with an automated radio telemetry system in a tropical rainfore st," *The Computer Journal*, vol. 54, no. 12, pp. 1931–1948, 2011.

[4] F. Dressler, S. Ripperger, M. Hierold, T. Nowak, C. Eibel, B. Cassens, F. Mayer, K. Meyer-Wegener, and A. Koelpin, "From radio telemetry to ultra-low power sensor networks - tracking bats in the wild," *IEEE Communications Magazine*, vol. 54, no. 1, pp. 129–135, 2016.

[5] I. Parvez, F. Abdul, and A. I. Sarwat, "A location based key management system for advanced metering infrastructure of smart grid," in *2016 IEEE Green Technologies Conference (GreenTech)*, pp. 62–67, April 2016.

[6] I. Iala, M. Ouadou, D. Aboutajdine, and O. Zytoune, "Energy based collision avoidance at the mac layer for wireless sensor network," in *2017 International Conference on Advanced Technologies for Signal and Image Processing (ATSIP)*, pp. 1–5, May 2017.

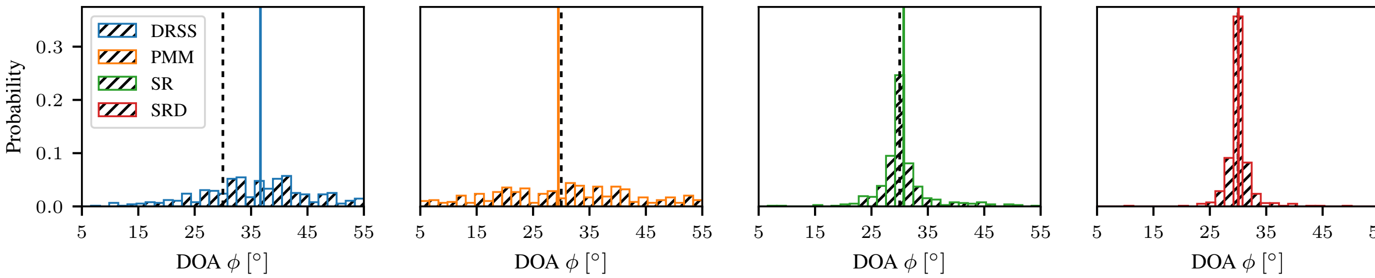

Fig. 7. Estimation results for a LOS angle of $\phi_{\mathrm{LOS}} = 30°$. The basic DRSS method for DOA estimation results in a significant bias. The PMM DOA estimates provide a zero-mean error. Though, with the PMM the variance of the DOA estimates is slightly increased. Thus, it is shown that incorporating prior channel knowledge enable unbiased DOA estimates at the cost of an increased variance. Both super-resolution techniques shown a substantial decrease in the DOA estimation variance while being unbiased. There is a marginal variance increase when the SR method is compared to the SRD as the spatial diversity of the SRD approach provides more robust delay estimates.

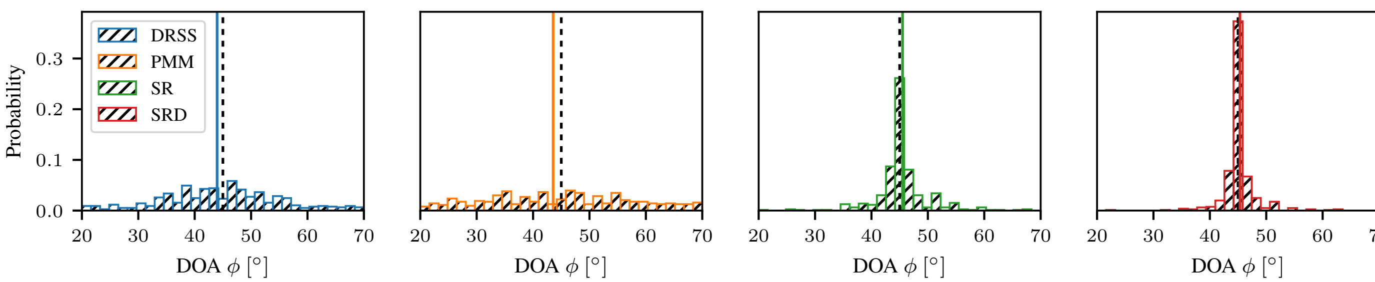

Fig. 8. Estimation results for a LOS angle of $\phi_{\mathrm{LOS}} = 45°$. For LOS angle of $\phi_{\mathrm{LOS}} = 45°$ the results are quite similar. However, results differ for the DRSS method which is not biased for $\phi_{\mathrm{LOS}} = 45°$. This is due to the fact that the gain difference function is symmetric and almost linear around 45°.

[7] T. Tuncer and B. Friedlander, eds., *Classical and Modern Direction-of-Arrival Estimation*. Academic Press, 2009.

[8] J. Ash and L. Potter, "Sensor network localization via received signal strength measurements with directional antennas," in *Proc. of the 2004 Allerton Conference on Communication, Control, and Computing*, pp. 1861–1870, 2004.

[9] T. Nowak, M. Hartmann, L. Patino-Studencki, and J. Thielecke, "Fundamental limits in rssi-based direction-of-arrival estimation," in *2016 13th Workshop on Positioning, Navigation and Communications (WPNC)*, pp. 1–6, Oct 2016.

[10] M. Malajner, P. Planinsic, and D. Gleich, "Angle of arrival estimation using rssi and omnidirectional rotatable antennas," *IEEE Sensors Journal*, vol. 12, pp. 1950–1957, June 2012.

[11] M. Malajner, D. Gleich, and P. Planinšič, "Angle of arrival measurement using multiple static monopole antennas," *IEEE Sensors Journal*, vol. 15, pp. 3328–3337, June 2015.

[12] B. N. Hood and P. Barooah, "Estimating doa from radio-frequency rssi measurements using an actuated reflector," *IEEE Sensors Journal*, vol. 11, pp. 413–417, Feb 2011.

[13] A. Cidronali, S. Maddio, G. Giorgetti, and G. Manes, "Analysis and performance of a smart antenna for 2.45-ghz single-anchor indoor positioning," *IEEE Transactions on Microwave Theory and Techniques*, vol. 58, pp. 21–31, Jan 2010.

[14] L. Kulas, "Simple 2-d direction-of-arrival estimation using an espar antenna," *IEEE Antennas and Wireless Propagation Letters*, vol. 16, pp. 2513–2516, 2017.

[15] R. Pohlmann, S. Zhang, T. Jost, and A. Dammann, "Power-based direction-of-arrival estimation using a single multi-mode antenna," in *2017 14th Workshop on Positioning, Navigation and Communications (WPNC)*, pp. 1–6, Oct 2017.

[16] M. Passafiume, S. Maddio, A. Cidronali, and G. Manes, "Music algorithm for rssi-based doa estimation on standard ieee 802.11/802.15. x systems," *World Sci. Eng. Acad. Soc. Trans. Signal Process*, vol. 11, pp. 58–68, 2015.

[17] T. Nowak, M. Hartmann, H. M. Tröger, L. Patino-Studencki, and J. Thielecke, "Probabilistic multipath mitigation in rssi-based direction-of-arrival estimation," in *2017 IEEE International Conference on Communications Workshops (ICC Workshops)*, pp. 1024–1029, May 2017.

[18] C. A. Balanis, *Modern Antenna Handbook*. New York, NY, USA: Wiley-Interscience, 2008.

[19] J. Proakis, *Digital communications*. Boston: McGraw-Hill, 2008.

[20] S. Jaeckel, L. Raschkowski, K. Börner, and L. Thiele, "Quadriga: A 3-d multi-cell channel model with time evolution for enabling virtual field trials," *IEEE Transactions on Antennas and Propagation*, vol. 62, pp. 3242–3256, June 2014.

[21] P. Stoica *et al.*, *Spectral Analysis of Signals*, vol. 452. Pearson Prentice Hall Upper Saddle River, 2005.

[22] R. Schmidt, "Multiple emitter location and signal parameter estimation," *IEEE Transactions on Antennas and Propagation*, vol. 34, pp. 276–280, Mar 1986.

[23] X. Li and K. Pahlavan, "Super-Resolution TOA Estimation With Diversity for Indoor Geolocation," *IEEE Transactions on Wireless Communications*, vol. 3, no. 1, pp. 224–234, 2004.

[24] S. U. Pillai and B. H. Kwon, "Forward/Backward Spatial Smoothing Techniques for Coherent Signal Identification," *IEEE Transactions on Acoustics, Speech, and Signal Processing*, vol. 37, no. 1, pp. 8–15, 1989.

[25] M. Wax and T. Kailath, "Detection of signals by information theoretic criteria," *IEEE Transactions on Acoustics, Speech, and Signal Processing*, vol. 33, pp. 387–392, Apr 1985.

[26] P. Stoica and Y. Selen, "Model-order selection: a review of information criterion rules," *IEEE Signal Processing Magazine*, vol. 21, pp. 36–47, July 2004.

[27] G. Xu *et al.*, "Detection of Number of Sources via Exploitation of Centro-Symmetry Property," *IEEE Transactions on Signal processing*, vol. 42, pp. 102–112, Januar 1994.

[28] T. Nowak and A. Eidloth, "Dynamic multipath mitigation applying unscented kalman filters in local positioning systems," in *Proc. European Wireless Technology Conf. (EuWIT)*, pp. 9–12, 2010.

[29] S. E. Bensley and B. Aazhang, "Subspace-based channel estimation for code division multiple access communication systems," *IEEE Transactions on Communications*, vol. 44, pp. 1009–1020, Aug 1996.